QUASI-STATIC ANALYSIS OF PLANAR TRANSMISSION LINES: CONFORMAL MAPPING VERSUS FINITE ELEMENTS

Milan DOLEŽAL, Zbyněk RAIDA
Dept. of Radio Electronics
Technical University of Brno
Purkyòova 118, 612 00 Brno
Czech Republic
E-mail: dolezal@urel.fee.vutbr.cz
raida@urel.fee.vutbr.cz

Abstract

The presented submission describes an analysis of a classical open microstrip line, of an open microstrip line on a trapezoidal substrate and on a substrate with a limited width and of a microstrip line with a PEC shielding walls on both sides. The analysis is performed using the conformal mapping method and the finite-element one. For all the above described structures, the characteristic impedance is computed by both the methods and obtained results are in detail discussed. Both the methods are compared with respect to their generality, to their CPU time requirements, and to the programming effort required for their implementation.

Keywords

Quasi-Static Analysis, Conformal Mapping, Finite Elements, Planar Transmission Lines

1. Introduction

The today's communication systems work on higher and higher frequencies. That is why the microwave and millimeter wave transmission lines play more and more important role in the today's radio electronics.

Dealing with the analysis of microwave and millimeter wave transmission lines, there are several numerical methods which were developed for this purpose because analytical solutions are not known [1].

Numerical methods can be divided into two groups:

Quasi-static methods come from the assumption that the dominant mode of the wave propagating longitudinally along the transmission line is well approximated by a TEM wave. Then, the transversal fields are very close to the static ones and they can be derived from a static potential solution of Laplace's equation [1]. The equation can be solved by the modified conformal mapping [2] [3], by the use of planar waveguide model [4] [5], by the finite-difference [6] or finite-element methods [7], by the use of a variational expression [8] [9] or an integral equation [10].

Since electromagnetic fields supported by microwave and millimeter-wave transmission lines have longitudinal components which are no more negligible at higher frequencies, fields have to be represented by a combination of TE and TM waves [1] and described by a vectorial wave equation which is the initial equation of the full-wave dynamic methods. The vectorial wave equation can be solved by the finite-difference [11] [12] or finite-element methods [13]-[16] or by the use of an analytical model of the transmission line [17].

If an analysis of a transmission line is going to be performed in the upper part of the microwave and millimeter-wave frequency range, full-wave dynamic methods have to be used because the quasi-static methods provide valid results typically below 5 GHz. On the other hand, the quasi-static methods are convenient to be used in the lower part of the microwave and millimeter-wave frequency range because they give in the described range of frequencies sufficiently accurate results, and moreover, they are in most cases simpler than full-wave methods.

The presented paper focuses on the quasi-static analysis of selected microstrip lines by the method of conformal mapping and by finite elements.

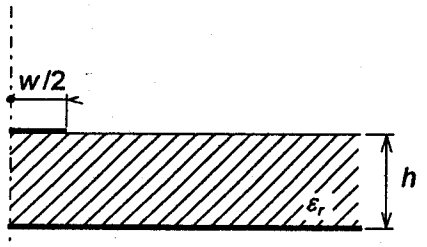

Fig. 1 An open microstrip line on a lossles isotropic substrate of the infinite extent. Negligible thickness of the PEC microstrip assumed.

In the section II, the principle of the conformal mapping is reviewed and both the so far published and the

newly developed closed-form algorithms for the analysis of various types of planar transmission lines are given. The section III presents a finite-element alternative to the conformal mapping solutions. Finally, the section IV brings the comparison of both the methods and describes hints for their use.

In all the paper, longitudinally homogenous structure exhibiting no losses (neither in the dielectrics nor in the metallic parts) are assumed. The substrate is supposed being isotropic, homogenous and linear. Moreover, the microstrip is assumed having infinitesimal thickness.

2. Conformal Mapping Method

The main idea of the conformal mapping method (CMM) consists in transforming a complicated electromagnetic field distribution and a complex structure geometry into a simple shape with a well-known field distribution. Moreover, if the propagation of a quasi-TEM wave is assumed, then microstrips and shielding walls can be considered as the electrostatic electrodes with a given potential and the characteristic impedances of a mapped and a mapping line are invariant.

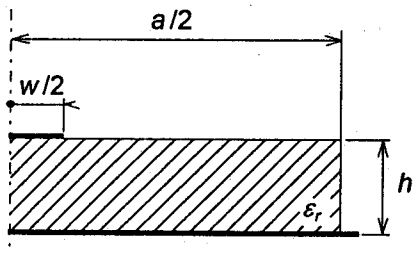

Fig. 2 An open microstrip line on a lossles isotropic substrate of a limited width. Negligible thickness of the PEC microstrip assumed.

The CMM analysis of an open microstrip line is well known for many years. In [2] and [18], the transmission structure was mapped into two straps eliminating the scattering fields. Moreover, both the straps had the same width (the width was called the effective one w_{ef}), which depended on the electrodes position and which was independent on the distribution of the dielectrics. The inhomogenous space between the straps was replaced then by a homogenous isotropic substrate with a relative effective permittivity $\varepsilon_{r,ef}$, representing the dielectric distribution. The distance between straps was denoted as h. Then, the characteristic impedance could be expressed by the relation [18]

$$Z_0 = \frac{120\pi}{\sqrt{\varepsilon_{ref}}} \cdot \frac{h}{w_{ef}} \qquad (1)$$

In order to compute the effective width w_{ef} of open microstrip lines on substrates of various shapes (Fig. 1, 2 and 4) and the relative effective permittivity $\varepsilon_{r,ef}$ of the classical open microstrip line (Fig. 1), the relations published in [18] have to be used. For the structures with limited substrates (Fig. 2, 4), new original relations [19] [20] were developed to calculate $\varepsilon_{r,ef}$ (see appendix A).

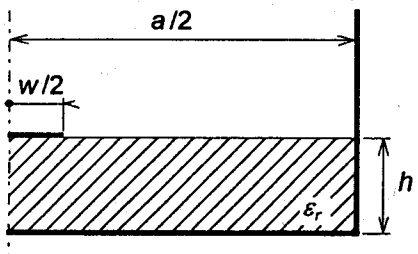

Fig. 3 An open microstrip line on a lossles isotropic substrate completed by PEC shielding walls on both sides. Negligible thickness of the PEC microstrip assumed.

Moreover, novel conformal transformations for wide and narrow microstrips shielded by side PEC walls (Fig. 3) were derived [21]. The method again consists in mapping a structure into two straps eliminating scattering field. New relations for computing w_{ef} and $\varepsilon_{r,ef}$ are given in the appendix A. The characteristic impedance can be determined by evaluating the relation (1).

3. Finite-Element Method

Assuming the propagation of the dominant quasi TEM wave along the microstrip structure enables to convert the electromagnetic problem into a electrostatic one [22]. Then, the electromagnetic field inside the structure can be described by the scalar electric potential φ and the structure can be analysed minimizing the energy functional [22]

$$F(\varphi) = \iint_S \varepsilon \nabla\varphi \cdot \nabla\varphi \, dS \qquad (2)$$

where ε denotes the permittivity inside the structure and the integration is performed over the cross section of the structure.

If the functional (2) is going to be minimized using the finite-element method, following three steps have to be performed:

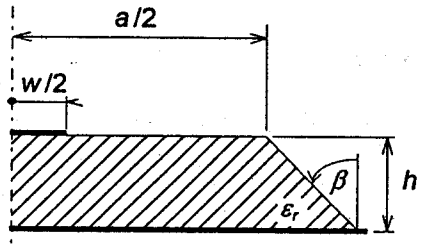

Fig. 4 An open microstrip line on a lossles isotropic trapezoidal substrate. Negligible thickness of the PEC microstrip assumed.

1. The cross section of the transmission line is subdivided into triangular finite elements (fig. 5). The finite-ele-

ment mesh is very dense near the microstrip where the electromagnetic field is concentrated, and therefore, dramatic changes of the potential can be supposed. Far from the microstrip, the size of the finite elements grows to reach efficiently such a distance from the microstrip in which the value of the potential can be neglected, and therefore, the structure can be then surrounded by a surface with the zero boundary condition (the potential of the microstrip is considered being one). Absorbing boundary conditions [23] or perfectly matched layers [24]-[31] have not been explored in the analysis because our experiments with them did not exhibit any significant improvement both in the CPU requirements and in the accuracy for the examined structures.

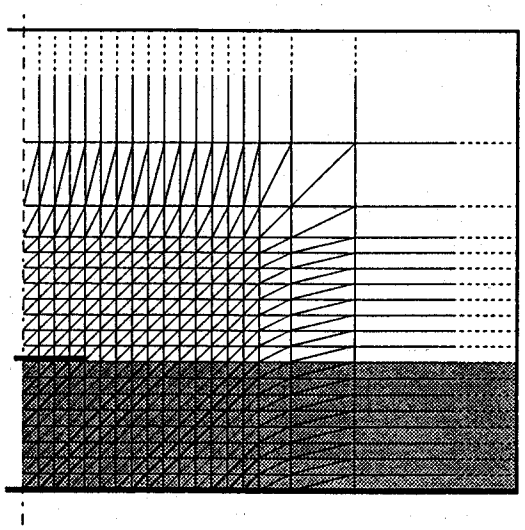

Fig. 5 An example of the architecture of the finite-element mesh used for the analysis of described microstrip transmission lines.

2. The potential distribution over a finite element is approximated using unknown nodal values of the potential φ_n and known shape functions based on the second-order Lagrange interpolation polynomials [22]:

$$\alpha_1 = 2\xi_1\left(\xi_1 - \tfrac{1}{2}\right) \quad (3a)$$

$$\alpha_2 = 4\xi_1\xi_2 \quad (3b)$$

$$\alpha_3 = 4\xi_3\xi_1 \quad (3c)$$

$$\alpha_4 = 2\xi_2\left(\xi_2 - \tfrac{1}{2}\right) \quad (3d)$$

$$\alpha_5 = 4\xi_2\xi_3 \quad (3e)$$

$$\alpha_6 = 2\xi_3\left(\xi_3 - \tfrac{1}{2}\right) \quad (3f)$$

In the above relations, ξ_i denote simplex coordinates (fig. 6). Using the above described shape functions, the approximation of the potential distribution over a finite element is described by the relation [22]

$$\tilde{\varphi} = \sum_{n=1}^{6} \alpha_n \varphi_n \quad (4)$$

The global approximation of the potential distribution over all the cross section of the investigated transmission line is obtained then by summing (4) of all the finite elements.

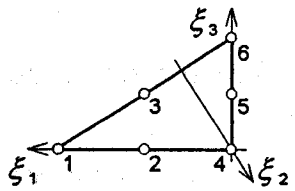

Fig. 6 Simplex coordinates and local nodes in the used triangular finite elements.

3. Substituting the global approximation into the functional (2), changing the order of summations and integrations, integrating products of shape-functions' derivatives and minimizing the resultant expression with respect to unknown nodal values yields the matrix equation [22]

$$\mathbf{D}\cdot\Phi = \Phi_n \quad (5)$$

In the above matrix equation, $\mathbf{D}$ is the global matrix consisting of coefficients obtained by integrating products of shape-functions' derivatives, Φ is the column vector of unknown nodal values of the potential and Φ_n denotes the column vector of the above described coefficients which are multiplied by known values of potentials from the boundaries.

If the matrix equation (5) is solved, then the unknown nodal values of the potential are obtained, and therefore, the approximation of the potential distribution over the cross section of the transmission line is yielded. Then, the electric intensity vector can be computed [1]

$$\mathbf{E} = -\nabla\varphi \quad (6)$$

and the charge per unitary length, which is accumulated on the microstrip, can be evaluated [1]

$$Q = \iint_S \mathbf{D}\cdot d\mathbf{S} \quad (7)$$

The integration is performed over a cylindrical surface surrounding the microstrip.

On the basis of the computed charge Q, the capacity of the structure per the unitary length C can be obtained. If the computation is repeated for the structure without the dielectric substrate and the capacity C_a is obtained then the characteristic impedance of the structure is given by [1]

$$Z_0 = Z_{0m}^a \sqrt{\frac{C_a}{C}} \quad (8)$$

with

$$Z_{0m}^a = \frac{1}{cC_a} \quad (9)$$

where c is velocity of light in the vacuum.

The above described algorithm has been implemented in matlab using the sparse matrix operations. By this way, high efficiency of the developed code has been reached.

4. Conformal Mapping versus Finite Elements

In this section, the above introduced methods are going to be in detail compared. The correspondence of obtained results for examined structures is the first point of view.

w [mm]	CM	FE	δ [%]
0,635	97,18	99,78	2,7
1,270	71,90	73,85	2,7
1,905	58,66	59,66	1,7
2,540	49,69	50,35	1,3

Tab. 1 Characteristic impedance of an open microstrip line of the width w and negligible thickness $t \approx 0$ on a lossles isotropic substrate (relative permittivity $\varepsilon_r = 4.2$, height $h = 1.27$ mm) of the infinite extent. The percentage error δ is related to the finite-element solution as the reference value.

w [mm]	CM	FE	δ [%]
0,635	82,57	83,76	1,4
1,270	55,21	56,30	2,0
1,905	37,94	38,36	1,1

$a = 2.54$ mm

w [mm]	CM	FE	δ [%]
0,635	95,49	97,87	2,5
1,270	70,23	71,95	2,4
1,905	56,74	57,73	1,7
2,540	47,70	48,35	1,4

$a = 7.62$ mm

a [mm]	CM	FE	δ [%]
1,5875	35,59	36,49	2,5
2,5400	55,24	56,30	1,9
3,8100	64,56	65,86	2,0
5,0800	68,00	69,46	2,1
6,3500	69,49	71,09	2,3
7,6200	70,23	71,95	2,4

$w = 1.27$ mm

Tab. 2 Characteristic impedance of an open microstrip line of the width w and negligible thickness $t \approx 0$ on a lossles isotropic substrate (relative permittivity $\varepsilon_r = 4.2$, height $h = 1.27$ mm) with shielding walls in the distance a. The percentage error δ is related to the finite-element solution as the reference value.

Dealing with the classical open microstrip line (tab. 1), the relative error falls down when the w/h ratio increases. Since the case $w/h = 1$ is considered as a critical one for the conformal mapping (the algorithm for $w/h < 1$ and the algorithm for $w/h > 1$ meet here with relatively low accuracy), a high relative error was expected here. A high error for $w/h < 1$ was rather surprising for us and it is further investigated at the present time. Nevertheless, the error never swapped the level of 3%.

w [mm]	CM	FE	δ [%]
0,635	104,03	102,68	-1,3
1,270	77,26	77,28	0,0
1,905	64,50	64,08	-0,7

$a = 2.54$ mm

w [mm]	CM	FE	δ [%]
0,635	99,00	99,83	0,8
1,270	73,13	73,90	1,1
1,905	60,14	59,72	-0,7
2,540	51,13	50,42	-1,4

$a = 7.62$ mm

a [mm]	CM	FE	δ [%]
1,5875	82,49	83,29	1,0
2,5400	77,26	77,28	0,0
3,8100	75,10	74,80	-0,4
5,0800	74,14	74,16	0,0
6,3500	73,56	73,97	0,6
7,6200	73,13	73,90	1,1

$w = 1.27$ mm

Tab. 3 Characteristic impedance of an open microstrip line of the width w and negligible thickness $t \approx 0$ on a lossles isotropic substrate (relative permittivity $\varepsilon_r = 4.2$, height $h = 1.27$ mm) with limited width a. The percentage error δ is related to the finite-element solution as the reference value.

In the case of a microstrip with side shielding PEC walls (tab. 2), the obtained results corresponds better with the above described consideration: the relative error reaches its maxim for the ration $w/h = 1$ for the short distance between shielding walls (a = 2,54 mm) and almost its maxim for the long one ($a = 7.62$ mm). Examining the influence of the distance between the shielding walls to the relative error for the worst case ($w/h = 1$), approximately the same error (about 2 per cent) was observed for whole the investigated range. As at the previous structure, the error never swapped the level of 3%.

The best coincidence between the CM results and the FE ones was obtained for the microstrip with the limited width of the substrate (tab.3). In this case, the relative error was mostly below 1 per cent and it never swapped the level of 2%. Moreover, the ratio $w/h = 1$ did not seem being critical and the relative error exhibited an irregular spread over all the investigated cases.

Finally, let's have a look at the microstrip line on a trapezoidal substrate (tab. 4). First, both the width of the microstrip w and the angle of the side of the substrate β

(fig. 4) were fixed and the width of the substrate a was changed (tab. 4). A very bad coincidence of results was observed for the case when the microstrip covered the whole upper side of the substrate (the relative error swapped 5%)[1]. In the opposite case (the microstrip did not cover the whole upper side of the substrate but its part only), the relative error was lower but it stays all the time relatively high (about 3%). At the present time, the cause of the described behaviour of our algorithms is intensively investigated.

Second, both the width of the microstrip w and the width of the substrate a were fixed and the angle of the side of the substrate β was changed. Then, the relative error stayed about 3% again.

a [mm]	CM	FE	δ [%]
1,270	75,47	79,32	5,1
2,540	75,32	76,88	2,1
3,810	74,32	76,17	2,5
5,080	73,75	75,97	3,0

$w = 1.27$ mm, $\beta = 45°$

β [deg]	CM	FE	δ [%]
60	73,57	75,93	3,2
20	73,98	76,05	2,8

$w = 1.27$ mm, $a = 5.08$ mm

Tab. 4 Characteristic impedance of an open microstrip line of the width w and negligible thickness $t \approx 0$ on a lossles isotropic trapezoidal substrate (width of the upper side a, relative permittivity $\varepsilon_r = 4.2$, height $h = 1.27$ mm). The percentage error δ is related to the finite-element solution as the reference value.

Searching for the sources of the above described relative errors, the accuracy of the conformal mapping method is influenced by the accuracy of used geometrical approximations, and therefore, searching for more suitable approximations can increase the accuracy of the method.

Dealing with the finite elements, the operator in the functional (2) is non-negative, and therefore the method converges in the sense of energy [32]. By other words, increasing the number of finite elements, into which the cross sections of investigated transmission lines are broken, or increasing the order of approximation functions yield increasing accuracy of the method. On the other hand, assuming zero potential in the high distance from the microstrip introduces an additional error into the method.

Dealing with the generality of developed algorithms, the conformal mapping requires an intellectual effort for obtaining an algorithm for the analysis of each type of the microstrip structure whereas the developed finite-element algorithm enables to analyse an arbitrary structure. On the other hand, higher computational requirements (the finite-element program consumes minutes of the CPU time on a workstation whereas the evaluating conformal mapping algorithms takes milliseconds on a regular PC) and a more difficult programming are the price, which finite elements have to pay for the advantage of their generality.

Dealing more in detail with the programming effort required for the implementation of the described algorithms, the conformal mapping provides closed-form formulas which can be very easily implemented on a few programming lines using standard mathematical operations and functions. On the other hand, the finite-element method requires a relatively complicated mesh generator and an efficient computational kernel, which is able to handle with sparse matrices. Moreover, the finite-element method is able to provide an information about the field distribution over the cross section of the investigated structure, and therefore, a graphical post processor, which visualises potential or field distribution over this cross section has to be implemented. Fortunately, most of the described functions belong to the basic core of matlab, and therefore, their implementation is not very difficult. On the other hand, conformal mapping requires a programming effort for each analysed structure whereas the finite-element program can be used for the analysis of an arbitrary structure without any change.

5. Conclusions

The presented paper compares the conformal mapping method with the finite-element one. Although both the methods are of the different nature (conformal mapping is based on the geometrical transform of complicated shapes and field distributions whereas finite elements come from the minimization of the energy functional), there is a good correspondence between obtained results. The best correspondence was achieved for the open microstrip line on a substrate width the limited with (the relative error did not swapped 2%), and the worst results were obtained for the open microstrip line on a trapezoidal substrate (the relative error reached 5% when the microstrip covered the whole upper side of the substrate).

The generality of the algorithm is the greatest advantage of finite elements: the developed program can be used for the analysis of a transmission line with an arbitrary structure whereas the conformal mapping requires an intellectual effort for every single structure. High CPU-time requirements are the price, which is paid for the generality of finite elements. That is why the enemies of finite elements say that users of finite-elements replace their intellectual insufficiency by the rough computational power. Users of finite element can oppose, that the computational power of computers very dramatically rises, and therefore,

[1] In this special case, an algorithm published in [19] was used; This special algorithm is not given in the appendix.

CPU-time requirements of finite-element programs rapidly fall down.

The presented paper bring arguments for both the sides of the above described quarrel. Therefore, it is up to reader to choose the method which is more suitable to him.

6. Acknowledgement

The project has been supported by the Grant Agency of the Czech Republic under the grant No. 102/97/1224: *„Design, analysis and optimization of special microwave structures"*.

7. Appendix

a) The CM algorithm for analysis of the classical open microstrip line on a substrate of the infinite extent (Fig. 1)

w ≥ h (use A.1; A.2 and A.36 to find out $\varepsilon_{r,ef}$)

$$w_{ef}=w+\frac{2h}{\pi}\ln\left[17.08\left(\frac{w}{2h}+0.85\right)\right] \tag{A.1}$$

$$S_0=\frac{h^2}{4}\operatorname{acosh}\left(\frac{\pi}{2}\frac{w_{ef}}{h}-1\right) \tag{A.2}$$

w<h (use A.3; A.4 and A.36 to find out $\varepsilon_{r,ef}$)

$$w_{ef}=\frac{2\pi h}{\ln\frac{8h}{w}} \tag{A.3}$$

$$S_0=\frac{h^2}{\ln^2\frac{8h}{w}}\left(\frac{\pi}{2}\ln\frac{8h}{w}-0.9\right) \tag{A.4}$$

b) The CM algorithm for the analysis of the open microstrip line on a substrate of a limited width (Fig. 2)

w ≥ h (use A.1; A.5; A.6; A.7; A.8; A.9; A.15; A.16; A.17; A.18 and A.36 to find out $\varepsilon_{r,ef}$)

$$u_e=\frac{h}{\pi}\operatorname{acosh}\left(\frac{\pi}{2}\frac{w_{ef}}{h}-1\right) \tag{A.5}$$

$$u_R\approx\frac{1}{2}\left(\sqrt{a^2+\frac{8}{\pi}hw_{ef}}-a\right)\left[1+\left(\frac{w}{a}\right)^{\sqrt{\frac{w}{h}}}\log\left(0.45+\frac{w}{h}\right)\right] \tag{A.6}$$

$$u_Q\approx\frac{1}{2}\left(1+\frac{w}{4a}\right)u_R \tag{A.7}$$

$$v_Q=\frac{h}{\pi}\operatorname{acos}\left[\frac{w_{ef}}{2}\frac{\sinh\left(u_Q\pi/h\right)}{a/2+u_Q}-\cosh\left(u_Q\frac{\pi}{h}\right)\right] \tag{A.8}$$

$$u_P=\frac{u_Q+\sqrt{u_Q^2+u_R\left(u_R-2u_Q\right)\left[1+\frac{h}{h-v_Q}\left(\frac{u_R-u_Q}{u_e}\right)^2\right]}}{1+\frac{h}{h-v_Q}\left(\frac{u_R-u_Q}{u_e}\right)^2} \tag{A.9}$$

w<h (use A.3; A.10; A.11; A.12; A.13; A.14; A.15; A.16; A.17; A.18 and A.36 to find out $\varepsilon_{r,ef}$)

$$u_e=\frac{h}{\ln(8h/w)}\operatorname{acos}\left(\frac{w}{8h}\right) \tag{A.10}$$

$$u_R=\frac{w_{ef}}{\pi}\operatorname{atan}\frac{2h}{a} \tag{A.11}$$

$$u_Q=\frac{u_R}{2} \tag{A.12}$$

$$v_Q=h-\frac{w_{ef}}{2\pi}\operatorname{acosh}\sqrt{1+\left(\frac{2h}{a}\right)^2} \tag{A.13}$$

$$u_P=\frac{2u_Q\left(h-v_Q\right)u_e^2}{hu_Q^2+\left(h-v_Q\right)u_e^2} \tag{A.14}$$

Now, for both cases **w<h** and **w ≥ h**

$$S_{01l}=u_Pv_Q+\frac{h-v_Q}{3}\left(u_Q+\frac{\left(u_P-u_Q\right)^3}{\left(u_R-u_Q\right)^2}\right) \tag{A.15}$$

$$S_{01P}=\frac{h}{3}\left(u_e-u_P\right)\left[2+\frac{u_P}{u_e}\left(2-\frac{u_P}{u_e}\right)\right] \tag{A.16}$$

$$S_{02}=\frac{2}{3}\left(h-v_Q\right)u_R \tag{A.17}$$

$$S_0=S_{01l}+S_{01P}+S_{02} \tag{A.18}$$

c) The CM algorithm for the analysis of the open microstrip line on a trapezoidal substrate (Fig. 4); $\theta=\pi/2-\beta$

w ≥ h (use A.1; A.5; A.6; A.7; A.8; A.9; A.15; A.16; A.17; A.19; A.20; A.23 and A.36 to find out $\varepsilon_{r,ef}$)

$$v_P=\frac{h}{\pi}\operatorname{acos}\left[\frac{w_{ef}}{2}\frac{\sinh\left(u_P\frac{\pi}{h}\right)}{a/2+u_P}-\cosh\left(u_P\frac{\pi}{h}\right)\right] \tag{A.19}$$

$$u_{R\Theta}\approx\frac{2h}{\pi}\operatorname{acotanh}\frac{2\left[\frac{a}{2}+h\operatorname{cotan}\Theta+\frac{2}{\pi}\Theta u_R\right]}{w_{ef}} \tag{A.20}$$

w<h (use A.3; A.10; A.11; A.12; A.13; A.14; A.15; A.16; A.17; A.21; A.22; A.23 and A.36 to find out $\varepsilon_{r,ef}$)

$$v_P=h-\frac{w_{ef}}{\pi}\operatorname{atanh}\left[\tan\left(\pi\frac{u_P}{w_{ef}}\right)\right] \tag{A.21}$$

$$u_{R\Theta}=\frac{w_{ef}}{\pi}\operatorname{atan}\left(\frac{2h\tan\Theta}{2h+a\tan\Theta}\right) \tag{A.22}$$

Now, for both cases **w<h** and **w ≥ h**

$$S_0=S_{01l}+S_{01p}+S_{02}-\frac{1}{2}(h-v_p)(u_R-u_{R\Theta}) \tag{A.23}$$

d) The CM algorithm for the analysis of the open microstrip line completed by PEC shielding walls on both sides (Fig.3)

w ≥ h (use A.24; A.25; A.26; A.27; A.28; A.29; A.35 and A.36 to find out $\varepsilon_{r,ef}$)

$$\frac{\pi}{2}(a-w)=a\operatorname{atan}\sqrt{\frac{\frac{a^2}{h^2}+2d}{d^2-2d}}-h\ln\frac{\left(\frac{a}{h}\sqrt{d^2-2d}-d\sqrt{\frac{a^2}{h^2}+2d}\right)^2}{2d\left(d^2+\frac{a^2}{h^2}\right)}$$

The above equation (A.24) is a transcendent relation for the parameter d which has to be looked for from it.

$$c=\sqrt{d^2-2d} \tag{A.25}$$

$$e=\sqrt{d^2+\frac{a^2}{h^2}} \tag{A.26}$$

$$w_{ef}\approx\frac{2h}{\pi}\left(2\ln\left(e\frac{h}{a}\right)+\frac{a}{2h}\left[\pi-\operatorname{acos}\left(1-\frac{2a^2}{e^2h^2}\right)\right]\right) \tag{A.27}$$

$$u_3=2\frac{h}{\pi}\operatorname{atanh}\frac{c}{d} \tag{A.28}$$

$$h=\frac{h}{\pi}\operatorname{acos}\left[\frac{\frac{a^2}{h^2}-\sqrt{A}}{2\cdot e^2}(\cosh U_p+1)\right]+ \tag{A.29}$$

$$+\frac{a}{2\pi}\ln\left(\frac{e^2\frac{\cosh U_p-1}{\cosh U_p+1}}{d^2-\sqrt{2}d\sqrt{\sqrt{A}+d^2-e^2\frac{\cosh U_p-1}{\cosh U_p+1}}+\sqrt{A}}\right)$$

$$A=\frac{a^4}{h^4}+4e^2\frac{d^2-\frac{a^2}{h^2}\cosh U_p}{(\cosh U_p+1)^2}$$

$$U_p=\pi\frac{u_p}{h}$$

The equation (A.29) is a transcendent relation for the parameter u_p which has to be looked for from it.

w<h (use A.30; A.31; A.32; A.33; A.34; A.35 and A.36 to find out $\varepsilon_{r,ef}$)

$$c=2h\frac{e^{\pi h/a}}{e^{2\pi h/a}-1} \tag{A.30}$$

$$w_p=4c\cos\left[\frac{\pi}{4}\left(2-\frac{w}{a}\right)\right]\cosh\left(\pi\frac{h}{a}\right) \tag{A.31}$$

$$w_{ef}=\frac{2\pi h}{\ln\left(8h/w_p\right)} \tag{A.32}$$

$$u_3=\frac{w_{ef}}{4}-0.068\left(\frac{w^2}{h}\right)\left(1-\frac{w}{a}\right)^2 \tag{A.33}$$

$$u_p=\frac{w_{ef}}{2\pi}\operatorname{acos}\frac{A^2-1}{A^2+1} \tag{A.34}$$

$$A=\frac{1+e^{2\pi h/a}}{2(h/c)e^{\pi h/a}}$$

Now, for both cases **w<h** and **w ≥ h**

$$S_0\approx\frac{1}{2}h(u_p+u_3)+\frac{1}{2}h\left(\frac{\pi}{2}-1\right)\left(1-\frac{u_p}{u_3}\right)^{\pi/2} \tag{A.35}$$

Relative effective permittivity ε_{ref} for all the structures can be evaluated according to the following relation on the basis of the known parameter S_0

$$\varepsilon_{ref}=1+\left(1-2\frac{S_0}{hw_{ef}}\right) \tag{A.36}$$

References

[1] GUPTA, K. C.- GARG, R.- BAHL, I.- BHARTIA, P.: "*Microstrip lines and slotlines*", 2/E, Artech House, Norwood, 1996.

[2] WHEELER, H. A.: "Transmission line properties of parallel wide strips by conformal mapping approximation", *IEEE Trans. on Microwave Theory Tech.*, vol. 12, no. 3, pp. 280-289, March 1964.

[3] WEN, C. P.: "Coplanar waveguide: a surface strip transmission line suitable for nonreciprocal gyromagnetic device application", *IEEE Trans. on Microwave Theory Tech.*, vol. 16, no. 12, pp. 1087-1090, December 1968.

[4] KOMPA, G.: "Dispersion measurement of the first two higher-order modes in open microstrip", *Arch. Elek. Ubertragung*, vol. 27, no. 4, pp. 182-184, April 1973.

[5] MEHRAN, R.: "The frequency-dependent scattering matrix of microstrip right angle bends", *Arch. Elek. Ubertragung*, vol. 29, no. 11, pp. 454-460, November 1975.

[6] VANDER VORST, A.: "Electromagnétisme - champs, forces et circuits", De Boeck-Wesmael, Bruxelles, 1990.

[7] SILVESTER, P.: "TEM wave properties of microstrip transmission lines", *Proc. of IEE*, vol. 115, pp. 43-48, January 1968.

[8] COLLIN, R. E.: "*Field theory of guided waves*", McGraw-Hill, New York, 1960.

[9] YAMASHITA, E.: "Variational method for the analysis of microstrip-like transmission lines", *IEEE Trans. on Microwave Theory Tech.*, vol. 16, no. 8, pp. 529-535, August 1968.

[10] HARRINGTON, R. F.: "*Field computation by moment methods*", Macmillan, New York, 1968.

[11] HORNSBY, J. S.- GOPINATH, A.: "Numerical analysis of a dielectric-loaded waveguide with a microstrip line - finite-difference methods", *IEEE Trans. on Microwave Theory Tech.*, vol. 17, no. 9, pp. 684-690, September 1969.

[12] CORR, D. G.- DAVIES, J. B.: "Computer analysis of the fundamental and higher order modes in single and coupled microstrip", *IEEE Trans. on Microwave Theory Tech.*, vol. 20, no. 10, pp. 669-678, October 1972.

[13] DALY, P.: "Hybrid-mode analysis of microstrip by finite-elements methods", *IEEE Trans. on Microwave Theory Tech.*, vol. 19, no. 1, pp. 19-25, January 1971.

[14] HANO, M.: "Finite-element analysis of dielectric-loaded waveguides", *IEEE Trans. on Microwave Theory Tech.*, vol. 32, no. 10, pp. 1275-1279, October 1984.

[15] HAYATA, K.- KOSHIBA, M.- EGUCHI, M.- SUZUKI, M.: "Vectorial finite-element method without any spurious solutions for dielectric waveguiding problems using transverse magnetic-field component", *IEEE Trans. on Microwave Theory Tech.*, vol. 34, no. 11, pp. 1120-1123, November 1986.

[16] LEE, J. F.- SUN, D. K.- CENDES, Z. J.: "Full-wave analysis of dielectric waveguides using tangential vector finite-elements", *IEEE Trans. on Microwave Theory Tech.*, vol. 39, no. 8, pp. 669-678, August 1991.

[17] HUYNEN, I.- VANDER VORST, A.: "A new variational formulation, applicable to shielded and open multilayered transmission lines with gyrotropic non-hermitian lossy media and lossless conductors". *IEEE Trans. Microwave Theory Tech.*, vol. 42, no. 11, pp. 2107 - 2111, Nov. 1994.

[18] SVAČINA, J.: "Investigation of Hybrid Microwave Integrated Circuits by a Conformal Mapping Method", *Publications of Technical and Scientific Papers of the TU of Brno*, vol. A-46, Brno, 91.

[19] DOLEŽAL, M.- SVAČINA, J.: "An Improvement of the analytical method of analysis of a trapezoidal microstrip line", *Proceedings of Workshop CAD&CAE 97*, pp. 19-21, Pardubice, 1997.

[20] DOLEŽAL, M.- SVAČINA, J.: "Algorithm for analysis of limited microstrip lines". submitted to conference *Radioelektronika 98*, Brno, 1998.

[21] DOLEŽAL, M.- SVAČINA, J.: "A novel conformal transformation for analysis of multilayered side shielded microstrip lines". Submitted to conference *IWK'98*, Ilmenau, 1998

[22] SILVESTER, P. P.- FERRARI, R. F.: "*Finite elements for electrical engineers*", 3/E, Cambridge University Press, Cambridge, 1996.

[23] PANTIC-TANNER, Z.- MAVRONIKOLAS, G. - MITTRA, R.: "A numerical absorbing boundary condition for quasi TEM analysis of microwave transmission lines using the finite-element method", *Microwave and Optical Technology Letters*, vol. 9, no. 3, pp. 134 - 136, June 1995.

[24] BERENGER, J. P.: "A perfectly matched layer for the absorption of electromagnetic waves", *J. Computational Phys.*, vol. 114, no. 2, pp. 185 - 200, October 1994.

[25] CHEW, W. CH.- WEEDON, W. H.: "A 3D perfectly matched medium from modified Maxwell's equations with stretched coordinates", *Microwave Optical Technology Lett.*, vol. 7, no. 13, pp. 559 - 603, September 1994.

[26] KATZ, D. S.- THIELE, E. T.- TAFLOVE, A.: "Validation and extension to three dimensions of the Berenger PML absorbing boundary condition for FD-TD meshes", *IEEE Microwave Guided Wave Lett.*, vol. 4, no. 8, pp. 268 - 270, August 1994.

[27] RAPPAPORT, C. M.: "Perfectly matched absorbing boundary conditions based on anisotropic lossy mapping of space", *IEEE Microwave Guided Wave Lett.*, vol. 5, no. 3, pp. 90 - 92, March 1995.

[28] SACKS, Z. S.- KINGSLAND, D. M.- LEE, R.- LEE, J. F.: "A perfectly matched anisotropic absorber for use as an absorbing boundary condition", *IEEE Trans. Antennas Propagat.*, vol. 43, no. 12, pp. 1460 - 1463, December 1995.

[29] ZHAO, L.- CANGELLARIS, A. C.: "A general approach for the development of unsplit-field time-domain implementations of perfectly matched layers for FDTD grid truncation", *IEEE Microwave Guided Wave Lett.*, vol. 6, no. 5, pp. 209 -211, May 1996.

[30] FANG, J.- WU, Z.: "Generalized perfectly matched layer for the absorption of propagating and evanescent waves in lossless and lossy media", *IEEE Trans. Microwave Theory Tech.*, vol. 44, no. 12, pp. 2216 - 2222, December 1996.

[31] GRIBBONS, M. A.- PINELLO, W. P.- CANGELLARIS, A. C.: "A stretched coordinate technique for numerical absorption of evanescent and propagating waves in planar waveguiding structures", *IEEE Trans. Microwave Theory Tech.*, vol. 43, no. 12, pp. 2883 - 2889, December 1995.

[32] DUDLEY, D. G.: "*Mathematical foundations for electromagnetic theory*", IEEE Press, Piscataway, 1994.

About authors...

Milan DOLEŽAL was born in 1972 in Brno. He received Ing. (M.S.) degree in Radio Electronics in 1995 at the Technical University of Brno. He is PhD. student at the Institute of Radio Electronics TU Brno now. He tries to analyse Planar Transmission Lines using a Conformal Mapping Method.

Zbyněk RAIDA was born in 1967 in Opava. He received Ing. (M.S.) degree in Radio Electronics in 1991 and Dr. (PhD.) degree in Electronics in 1994, both at the Technical University of Brno. Since 1993, he is with the Institute of Radio Electronics TU Brno where he works as an assistant professor. In 1996, he spent 6 months on leave at the Université Catholique de Louvain, Laboratoire de Hyperfrequences, Louvain-la-Neuve in Belgium. His teaching and research interest include adaptive filtering and artificial intelligence, numerical modelling of microwave circuits and antennas, object oriented programming and related topics.